PAPER

Diffusive spatial movement with memory and maturation delays

IOP Publishing | London Mathematical Society Nonlinearity

Nonlinearity **32** (2019) 3188–3208 https://doi.org/10.1088/1361-6544/ab1f2f

Diffusive spatial movement with memory and maturation delays

Junping Shi[1], **Chuncheng Wang**[2,4] **and Hao Wang**[3]

[1] Department of Mathematics, College of William and Mary, Williamsburg, VA 23187-8795, United States of America
[2] Department of Mathematics, Harbin Institute of Technology, Harbin, Heilongjiang 150001, People's Republic of China
[3] Department of Mathematical and Statistical Sciences, University of Alberta, Edmonton, AB T6G 2G1, Canada

E-mail: wangchuncheng@hit.edu.cn

Received 21 August 2018, revised 16 January 2019
Accepted for publication 3 May 2019
Published 26 July 2019

Recommended by Professor Guido Schneider

Abstract

A single species spatial population model that incorporates Fickian diffusion, memory-based diffusion, and reaction with maturation delay is formulated. The stability of a positive equilibrium and the crossing curves in the two-delay parameter plane on which the characteristic equation has purely imaginary roots are studied. With Neumann boundary condition, the crossing curve that separates the stable and unstable regions of the equilibrium may consist of two components, where spatially homogeneous and inhomogeneous periodic solutions are generated through Hopf bifurcation respectively. This phenomenon rarely emerges from standard partial functional differential equations with Neumann boundary condition, which indicates that the memory-based diffusion can induce more complicated spatiotemporal dynamics.

Keywords: memory-based diffusion, reaction diffusion equations, Hopf bifurcation, spatiotemporal dynamics
Mathematics Subject Classification numbers: 35B35, 37G10, 92D25

(Some figures may appear in colour only in the online journal)

[4] Author to whom any correspondence should be addressed.

1. Introduction

Reaction–diffusion equations have been widely used in mathematical modeling of many disciplines, such as physics, chemistry and biology [6, 17, 19]. Fickian diffusion, the most commonly used form of diffusion, assumes that the flux is proportional to the gradient of the concentration of the element. However, this is sometimes insufficient for realistically describing animal movements, especially for highly developed animals, since most animals have cognition and memory. A recent review paper [8] emphasized the significance of integrating spatial memory into the modeling of animal movements, and the memory-based diffusion is extremely complicated and poorly understood. In [23], we first modeled the episodic-like spatial memory of animals and formulated the following mathematical model by considering a directed movement toward the negative gradient of density distribution function at past time:

$$\begin{cases} \frac{\partial u}{\partial t} = D_1 \Delta u + D_2 \operatorname{div}(u \nabla u_\tau) + g(u), & x \in \Omega, t > 0, \\ \frac{\partial u}{\partial n}(t,x) = 0, & x \in \partial\Omega, t > 0. \end{cases} \tag{1.1}$$

Here $u = u(t,x)$, $u_\tau = u(t-\tau,x)$; Ω is a bounded domain in $\mathbb{R}^N$ ($N \geqslant 1$) with a smooth boundary $\partial\Omega$; a homogeneous Neumann boundary condition is imposed so that there is no population movement across the boundary $\partial\Omega$. It has been shown in [23] that the stability of a spatially homogeneous steady state fully depends on the relationship between the two diffusion coefficients but is independent of time delay.

For (1.1), the reaction term, including both birth and death processes, is considered to occur instantaneously. In the biological literature [12, 14, 17, 26], time delays are often incorporated in the process of modelling, for taking into account such factors like migration, diffusion of populations, gestation and maturation periods. In this paper, we shall consider a time delay in reaction term say σ, to account for renewable resources or animals to reach maturity. Such maturation delay can be incorporated as in the following model:

$$\begin{cases} \frac{\partial u}{\partial t} = D_1 \Delta u + D_2 \operatorname{div}(u \nabla u_\tau) + g(u, u_\sigma), & x \in \Omega, t > 0, \\ \frac{\partial u}{\partial n}(t,x) = 0, & x \in \partial\Omega, t > 0. \end{cases} \tag{1.2}$$

For $D_2 = 0$, the model reduces to a standard partial functional differential equation, which has been extensively studied in the literature. For Hopf bifurcation problems of (1.2) with $D_2 = 0$, the theoretical framework has been established in [31], and the detailed analyses for different choices of g are nontrivial [16, 35]. However, the stable periodic solutions generated through Hopf bifurcation are usually homogeneous for $D_2 = 0$, since the associated purely imaginary roots are usually derived from the characteristic equation of the corresponding delay system without diffusion. This is also the case for most such models described by parabolic equations with or without delays, see an example in [34]. It should be pointed out that Dirichlet boundary condition or higher-codimension bifurcation, such as Turing–Hopf bifurcation, may give rise to stable spatially inhomogeneous periodic solutions, see [2–5, 10, 25, 27, 28, 33].

In this paper, the stability and bifurcation analysis of a positive spatially homogeneous equilibrium u^* of (1.2) are investigated by analyzing the characteristic equation of the corresponding linearized equation. Since there are two independent delays involved in the equation, we employ a geometric method, developed in [11], to study the roots of a transcendental equation with two delays. The equilibrium is assumed to be stable when there are no memory-based diffusion and maturation delay ($D_2 = 0$ and $\sigma = 0$). The results in this paper reveal that, when the strength of the memory-based diffusion is strong compared with the Fickian diffusion ($|D_2|u^* \geqslant D_1$), then the equilibrium u^* is always unstable regardless of the maturation

delay σ and the movement delay τ, which generalizes earlier results in [23] for the case of $\sigma = 0$. On the other hand, when the memory-based diffusion is weak compared with the Fickian diffusion ($|D_2|u^* < D_1$), the equilibrium u^* remains stable for certain values of the delay pair (τ, σ), and the set of such values (stable parameter region) Θ is an open subset of $\mathbb{R}^2_+ = \{(\tau, \sigma) : \tau \geqslant 0, \sigma \geqslant 0\}$. The intrinsic growth rates play a more important role here: for some case, $\Theta = \mathbb{R}^2_+$, that is, the equilibrium remains stable for all possible delays; while for other cases, Θ is a true subset of $\mathbb{R}^+_2$, and stability switches of the equilibrium occur when the the parameter (τ, σ) moves across the boundary of Θ (crossing curves). Such stability switches is an indication of emergence of time-oscillatory patterns through Hopf bifurcations. We characterize the set Θ and its boundary for all possible cases. Most interestingly, we identify conditions on the pairs of delay values (τ, σ), diffusion coefficients (D_1, D_2) and growth rates which produce spatiotemporal oscillatory patterns–periodic in time and non-constant in space.

The above result provides a new mechanism of generating spatiotemporal oscillatory patterns with a combination of memory-based diffusion and maturation delay. Our earlier results in [23] show that the memory-based diffusion alone does not induce instability, and the stability of u^* depends on D_2 but not τ. In the absence of memory-based diffusion, the maturation delay can only produce a spatially homogeneous time-periodic patterns [16, 35]. Here we find that a proper combination of the two delay mechanisms can produce spatially inhomogeneous time-periodic patterns. Note that multiple stability switches are known for some systems with two delays, but all previous studies are for non-spatial models [1, 13, 15, 18, 21, 22, 30, 32]. This paper appears to be the first study of a two-delay problem with one delay in the spatial dispersal part and the other one in the birth/death part of the model. Also all these previous work only produce oscillatory patterns without spatial structure, while spatiotemporal patterns are found here.

The paper is organized as follows. In the next section, we first prove the well-posedness of model (1.2), and we also prove the principle of linearized stability so that the linear stability implies nonlinear stability. We then study the distribution of the roots to the characteristic equation associated with (1.2), and find the crossing curves on which the characteristic equation has purely imaginary roots. In section 3, we apply the results to a diffusive Wright–Hutchinson equation and its variants, and we obtain crossing curves for generating spatially homogeneous and inhomogeneous periodic solutions. We discuss our model and results in section 4. Throughout the paper, $\mathbb{N}$ represents the set of all positive integers, and $\mathbb{N}_0 = \mathbb{N} \cup \{0\}$ represents the set of all non-negative integers.

2. Stability analysis

Throughout the paper, we assume that the initial condition $\phi(t, x)$ satisfies

$$\phi(t,x) \in C^{2,\alpha}([-\max\{\tau,\sigma\}, 0] \times \overline{\Omega}), \quad \frac{\partial \phi}{\partial n}(t,x) = 0, \quad (t,x) \in [-\max\{\tau,\sigma\}, 0] \times \partial\Omega, \alpha \in (0,1). \tag{2.1}$$

And the growth rate g in (1.2) is assumed to satisfy

($H1$) $g \in C^1([0,\infty) \times [0,\infty), \mathbb{R})$, $g(0,0) = 0$, $g(u, u_\sigma)/u$ is bounded, and $\exists u^*, \bar{u} > 0$ such that $g(u^*, u^*) = 0$ and $g(u,u) < 0$ for $u > \bar{u}$.

($H2$) Denote $A = g_u(u^*, u^*)$ and $B = g_{u_\sigma}(u^*, u^*)$. Assume that $A + B < 0$. (Otherwise, the equilibrium u^* of $u' = g(u, u_\sigma)$ is always unstable).

First we have the following well-posedness result for solutions of (1.2).

Theorem 2.1. *Suppose that* $D_1 > 0$, $D_2 \in \mathbb{R}$ *and* $\tau, \sigma > 0$, $\phi(t,x)$ *satisfies (2.1) and* $g(u)$ *satisfies* $(H1)$. *Then, equation (1.2) possesses a unique solution* $u(t,x)$ *for* $(t,x) \in [0,\infty) \times \overline{\Omega}$. *Moreover if* $\phi(t,x) \geqslant 0$ *for* $(t,x) \in [-\max\{\tau,\sigma\}, 0] \times \partial\Omega$, *then* $u(t,x) > 0$ *for* $(t,x) \in [0,\infty) \times \overline{\Omega}$.

Proof. For $t \in [0, \min\{\tau,\sigma\}]$, u_τ and u_σ coincides with the initial function $\phi(t-\tau,x)$ and $\phi(t-\sigma,x)$, respectively. Set $F(u) = D_2 \operatorname{div}(u\nabla\phi(t-\tau,x)) + g(u,\phi(t-\sigma,x))$. It follows from [29, Proposition 7.3.3] that (1.2) has a unique solution $u \in C^{2,1}(\bar{\Omega} \times [0,T))$ for some $T > 0$. The condition $g(u,u) < 0$ for $u > \bar{u}$ guarantees that the solution can be extended to $[0, \min\{\tau,\sigma\}]$ if $\min\{\tau,\sigma\} > T$. Then this process can be repeated to $[k\min\{\tau,\sigma\}, (k+1)\min\{\tau,\sigma\}]$ for $k \in \mathbb{N}$ as the step method for the existence of solutions to delay differential equations. Thus the solution can be extended to $t \in [0,\infty)$.

To show that the solution $u(t,x)$ is positive, we observe that u is the solution of the initial-boundary value problem:

$$\begin{cases} \frac{\partial u}{\partial t} = D_1\Delta u + D_2 \operatorname{div}(u\nabla_x\phi(t-\tau,x)) + g(u,\phi(t-\sigma,x)), & x \in \Omega, 0 < t < \min\{\tau,\sigma\}, \\ \frac{\partial u}{\partial n}(t,x) = 0, & x \in \partial\Omega, t > 0, \\ u(0,x) = \phi(0,x), & x \in \Omega. \end{cases} \tag{2.2}$$

Since $g(u,\phi(t-\sigma,x))/u$ is bounded, it then follows from maximum principle of parabolic equations that $u(t,x) > 0$ for $(t,x) \in (0, \min\{\tau,\sigma\}) \times \overline{\Omega}$. Repeating this argument, we obtain that $u(t,x) > 0$ for $(t,x) \in (0,\infty) \times \overline{\Omega}$. □

The linearized equation of (1.2) at a constant equilibrium solution u^* is

$$\frac{\partial v}{\partial t} = D_1\Delta v + D_2u^*\Delta v(t-\tau,x) + Av + Bv(t-\sigma,x). \tag{2.3}$$

Define the real-valued Sobolev space X by

$$X = \left\{ u \in H^2(\Omega) : \frac{\partial u}{\partial n} = 0,\ x \in \partial\Omega \right\},$$

and the complexification of X is given by

$$X_{\mathbb{C}} = X \oplus \mathrm{i}X = \{x_1 + \mathrm{i}x_2 : x_1, x_2 \in X\}.$$

By assuming that $v(t,x) = \mathrm{e}^{\mu t}y(x)$, we obtain that the characteristic equation of (2.3) is given by

$$\mu y - D_1\Delta y - D_2u^*\mathrm{e}^{-\mu\tau}\Delta y - Ay - B\mathrm{e}^{-\mu\sigma}y = 0, \tag{2.4}$$

where $0 \neq y \in X_{\mathbb{C}}$ and $\mu \in \mathbb{C}$. It follows from lemma 3.1 in [23] that (2.4) is equivalent to a family of transcendental equations with μ as eigenvalues:

$$E(n,\tau,\sigma,\mu) := \mu + D_1\lambda_n - A + D_2u^*\lambda_n\mathrm{e}^{-\mu\tau} - B\mathrm{e}^{-\mu\sigma} = 0,\ n \in \mathbb{N}_0 \tag{2.5}$$

where λ_n are eigenvalues of

$$\begin{cases} \Delta\phi + \lambda\phi = 0, & x \in \Omega, \\ \frac{\partial\phi}{\partial n}(x) = 0, & x \in \partial\Omega, \end{cases} \tag{2.6}$$

satisfying $0 = \lambda_0 < \lambda_1 \leqslant \lambda_2 \leqslant \cdots \leqslant \lambda_n \leqslant \cdots$ and $\lim_{n\to\infty} \lambda_n = \infty$. By a similar argument as the proof of theorem 3.4 in [23], we have the following conclusion on the principle of linearized stability of (1.2).

Theorem 2.2. *Assume that $D_1 > |D_2|u^*$. Then, the zero solution of (2.3) is asymptotically stable if all the roots of (2.5) have strictly negative real parts.*

Proof. For (2.3), we make the following change of variable

$$D_1 v(t,x) + D_2 u^* v(t-\tau,x) = w(t,x).$$

Then,

$$v(t,x) = \frac{1}{D_1}\sum_{n=0}^{\infty}(-1)^n q^n w(t-n\tau,x) := \frac{1}{D_1}\mathcal{D}w_t(\cdot,x) \tag{2.7}$$

where $q = \frac{D_2 u^*}{D_1}$. Substituting (2.7) into (2.3), we have the following linear neutral partial functional differential equation with an infinite number but countably many delays:

$$\frac{\partial \mathcal{D}w_t(\cdot,x)}{\partial t} = D_1 \Delta w(t,x) + \bar{\mathcal{D}}w_t(\cdot,x) \tag{2.8}$$

where

$$\bar{\mathcal{D}}w_t(\cdot,x) = \sum_{n=0}^{\infty}(-1)^n q^n [Aw(t-n\tau,x) + Bw(t-n\tau-\sigma,x)].$$

Therefore, the statement will follow from a similar argument as the proof of theorem 3.4 in [23]. □

To gain information on the set of roots of (2.5), we make the following definitions. For any $n \in \mathbb{N}_0$, $\tau \geqslant 0$ and $\sigma \geqslant 0$, denote

$$\Sigma_n(\tau,\sigma) = \{\mu \in \mathbb{C} : E(n,\tau,\sigma,\mu) = 0\}.$$

We say that $u = u^*$ is stable in mode-n if $\Sigma_n(\tau,\sigma) \subseteq \mathbb{C}^-$, and $u = u^*$ is stable if the spectral set $\Sigma(\tau,\sigma) \equiv \bigcup_{n=0}^{\infty}\Sigma_n(\tau,\sigma) \subseteq \mathbb{C}^-$, where $\mathbb{C}^- = \{a + b\mathrm{i} \in \mathbb{C} : a < 0, b \in \mathbb{R}\}$. We also define the mode-n stable parameter region to be

$$\Theta_n = \{(\tau,\sigma) : \tau \geqslant 0, \sigma \geqslant 0, \Sigma_n(\tau,\sigma) \subseteq \mathbb{C}^-\}, \tag{2.9}$$

and $\Theta = \bigcap_{n=0}^{\infty}\Theta_n$ is the stable parameter region in the (τ,σ)-plane. The boundary Π_n of Θ_n are curves on which (2.5) has purely imaginary or zero roots (called crossing curves in the literature), which is denoted by

$$\Pi_n = \{(\tau,\sigma) : \tau \geqslant 0, \sigma \geqslant 0, \Sigma_n(\tau,\sigma) \subseteq \mathbb{C}^0\}. \tag{2.10}$$

Here, $\mathbb{C}^0 = \{b\mathrm{i} \in \mathbb{C} : b \in \mathbb{R}\}$ represents the imaginary axis. For any $(\tau,\sigma) \in \Pi_n$, there exists $\omega \in \mathbb{R}^+$ such that $E(n,\tau,\sigma,\pm\mathrm{i}\omega) = 0$. For any $n \in \mathbb{N}_0$, we define

$$\Omega_n = \{\omega \in \mathbb{R}^+ : E(n,\tau,\sigma,\pm\mathrm{i}\omega) = 0, (\sigma,\tau) \in \Pi_n\}. \tag{2.11}$$

Note that under the assumption $(H2)$, $\mu = 0$ is not a root of (2.5) for any $\tau \geqslant 0$, $\sigma \geqslant 0$.

When $n = 0$, the equation (2.5) is reduced to a single delay situation as $\lambda_0 = 0$, then the following conclusion is a direct consequence of theorem 4.7 in [26].

Proposition 2.3.

(1) If $A + B < 0$ and $B \geqslant A$, then all the roots of (2.5) with $n = 0$ have strictly negative real parts, that is, $\Theta_0 = \{(\tau, \sigma) : \tau \geqslant 0, \sigma \geqslant 0\}$;
(2) If $A + B < 0$ and $B < A$, then there exists $\sigma_0 > 0$ such that all the roots of (2.5) with $n = 0$ have strictly negative real parts when $0 \leqslant \sigma < \sigma_0$, and there exists a pair of purely imaginary roots for (2.5) with $n = 0$ at σ_0 while all the other roots have strictly negative real parts, that is, $\Theta_0 = \{(\tau, \sigma) : \tau \geqslant 0, 0 \leqslant \sigma < \sigma_0\}$.

When $n \geqslant 1$, (2.5) is a transcendental equation with two distinct time delays. For such equation, in order to seek the crossing curve Π_n on (τ, σ)-plane on which (2.5) has purely imaginary roots, we follow the geometric method proposed in [9]. We shall show that the crossing curves Π_n can be parameterized by $\omega \in \Omega_n$. For that purpose, we first determine the admissible frequency set Ω_n. Let

$$A_n = D_1\lambda_n - A, \quad \text{and} \quad B_n = D_2u^*\lambda_n.$$

Proposition 2.4. *Let Θ_n, Π_n and Ω_n be defined as in (2.9)–(2.11).*

(1) When $|B_n| + |B| < |A_n|$, $\Omega_n = \emptyset$; in particular, if $D_1 > |D_2|u^*$, then $\Omega_n = \emptyset$ for large n.
(2) When $|B_n| + |B| > |A_n|$, if $-|A_n| < |B_n| - |B| < |A_n|$, then $\Omega_n = (0, \omega_n^r]$; if $|B_n| - |B| > |A_n|$ or $|B_n| - |B| < -|A_n|$, then $\Omega_n = [\omega_n^l, \omega_n^r]$, where $\omega_n^r = \sqrt{(|B_n| + |B|)^2 - A_n^2}$ and $\omega_n^l = \sqrt{(|B_n| - |B|)^2 - A_n^2}$. In particular, if $D_1 < |D_2|u^*$, then ω_n^l and ω_n^r also satisfy

$$\lim_{n\to\infty} \omega_n^l = \lim_{n\to\infty} \omega_n^r = \infty, \quad \lim_{n\to\infty} (\omega_n^r - \omega_n^l) = \frac{2|D_2u^*B|}{\sqrt{(D_2u^*)^2 - D_1^2}}. \tag{2.12}$$

Proof. Denote

$$a_1^n(\mu) = \frac{B_n}{A_n + \mu}, \quad a_2^n(\mu) = \frac{-B}{A_n + \mu}.$$

Then (2.5) is equivalent to

$$a^n(\mu, \tau, \sigma) := 1 + a_1^n(\mu)\mathrm{e}^{-\mu\tau} + a_2^n(\mu)\mathrm{e}^{-\mu\sigma} = 0. \tag{2.13}$$

Define

$$F_1^n(\omega) := |a_1^n(\mathrm{i}\omega)| + |a_2^n(\mathrm{i}\omega)| = \frac{|B_n| + |B|}{\sqrt{A_n^2 + \omega^2}} \geqslant 0,$$
$$F_2^n(\omega) := |a_1^n(\mathrm{i}\omega)| - |a_2^n(\mathrm{i}\omega)| = \frac{|B_n| - |B|}{\sqrt{A_n^2 + \omega^2}}.$$

By proposition 3.1 in [9], the admissible value of ω, for which $\pm\mathrm{i}\omega$, $\omega \neq 0$ are purely imaginary roots of (2.5) for some $\tau, \sigma > 0$, must satisfy

$$F_1^n(\omega) \geqslant 1, \quad -1 \leqslant F_2^n(\omega) \leqslant 1 \tag{2.14}$$

that is, $\Omega_n = \{\omega \in \mathbb{R}^+ : F_1^n(\omega) \geqslant 1, -1 \leqslant F_2^n(\omega) \leqslant 1\}$.

(1) When $|B_n| + |B| < |A_n|$, then $F_1^n(0) < 1$. Since $F_1^n(\omega) > 0$ and $F_1^n(\omega)$ is strictly decreasing to 0 as $\omega \to \infty$, we have $F_1^n(\omega) < 1$ for all $\omega \geqslant 0$, which violates the first inequality of (2.14). Therefore, $\Omega_n = \emptyset$. When $D_1 > |D_2|u^*$, we get $|B_n| + |B| < |A_n|$ for large n. It then follows that $\Omega_n = \emptyset$ for large n.

(2) When $|B_n| + |B| > |A_n|$, $F_1^n(0) > 1$ and $F_1^n(\omega) = 1$ has a unique positive root $\omega_n^r = \sqrt{(|B_n| + |B|)^2 - A_n^2}$, such that $F_1^n(\omega) \geqslant 1$ for $\omega \in [0, \omega_n^r]$. If in addition $-|A_n| < |B_n| - |B| < |A_n|$, we have $-1 \leqslant F_2^n(0) \leqslant 1$. As $\omega \to \infty$, $F_2^n(\omega)$ is strictly decreasing to 0 when $|B_n| > |B|$, and increasing to 0 when $|B_n| < |B|$. It then follows that $-1 \leqslant F_2^n(\omega) \leqslant 1$ for all $\omega \geqslant 0$. Therefore, $\Omega_n = (0, \omega_n^r]$ in this case, since ω is not allowed to take 0, as discussed in [9].

On the other hand if $|B_n| - |B| > |A_n|$, we know that $|B_n| > |B|$ and $F_2^n(0) > 1$. By the monotonicity of $F_2^n(\omega)$, it follows that $F_2^n(\omega) = 1$ also has a unique positive root $\omega_n^l = \sqrt{(|B_n| - |B|)^2 - A_n^2}$, such that $0 < F_2^n(\omega) \leqslant 1$ for $\omega \in [\omega_n^l, \infty]$. Since $F_1^n(\omega) \geqslant F_2^n(\omega)$ for $\omega \geqslant 0$, we have $\omega_n^l < \omega_n^r$. Thus, $\Omega_n = [\omega_n^l, \omega_n^r]$. For the case of $|B_n| - |B| < -|A_n|$, one can also prove the statement by a similar argument.

As a special case, if $D_1 < |D_2|u^*$, it then follows from $\lim_{n\to\infty} \lambda_n = \infty$ that

$$|B_n| \pm |B| = |D_2|u^* \lambda_n \pm |B| > |D_1\lambda_n - A| = |A_n|$$

for large n. Hence, $\Omega_n = [\omega_n^l, \omega_n^r]$ for large n. From $F_2^n(\omega_n^l) = 1$ and $F_1^n(\omega_n^r) = 1$, we have

$$\begin{aligned} |D_2u^*\lambda_n|^2 + B^2 - 2|D_2u^*\lambda_n B| &= (D_1\lambda_n - A)^2 + (\omega_n^l)^2, \\ |D_2u^*\lambda_n|^2 + B^2 + 2|D_2u^*\lambda_n B| &= (D_1\lambda_n - A)^2 + (\omega_n^r)^2. \end{aligned} \tag{2.15}$$

Dividing (2.15) by λ_n^2 on both sides, and passing $n \to \infty$, this yields

$$\lim_{n\to\infty} \frac{\omega_n^l}{\lambda_n} = \lim_{n\to\infty} \frac{\omega_n^r}{\lambda_n} = \sqrt{(D_2u^*)^2 - D_1^2}. \tag{2.16}$$

Using (2.15) again, we have $(\omega_n^r)^2 - (\omega_n^l)^2 = 4|D_2u^*\lambda_n B|$, which, together with (2.16), implies the second limit in (2.12). □

Whenever the set Ω_n is nonempty, one can define

$$\begin{aligned} \theta_1^n(\omega) &= \arccos\left(\frac{1 + |a_1^n(\mathrm{i}\omega)|^2 - |a_2^n(\mathrm{i}\omega)|^2}{2|a_1^n(\mathrm{i}\omega)|}\right), \\ \theta_2^n(\omega) &= \arccos\left(\frac{1 + |a_2^n(\mathrm{i}\omega)|^2 - |a_1^n(\mathrm{i}\omega)|^2}{2|a_2^n(\mathrm{i}\omega)|}\right) \end{aligned}$$

for $\omega \in \Omega_n$. From proposition 4.5 in [9], for any $n \geqslant 1$, the mode-n crossing curve of (2.5) is

$$\Pi_n = \bigcup \mathcal{T}_{n,p,q}^{\pm}(\omega) := \{(\tau_{n,p}^{\pm}(\omega), \sigma_{n,q}^{\pm}(\omega)) : \omega \in \Omega_n\},$$

where

$$\begin{aligned} \tau_{n,p}^{\pm}(\omega) &= \frac{\angle a_1^n(\mathrm{i}\omega) + (2p-1)\pi \pm \theta_1^n(\omega)}{\omega},\ p = p_{0,n}^{\pm}, p_{0,n}^{\pm} + 1, p_{0,n}^{\pm} + 2, \cdots, \\ \sigma_{n,q}^{\pm}(\omega) &= \frac{\angle a_2^n(\mathrm{i}\omega) + (2q-1)\pi \mp \theta_2^n(\omega)}{\omega},\ q = q_{0,n}^{\pm}, q_{0,n}^{\pm} + 1, q_{0,n}^{\pm} + 2, \cdots, \end{aligned} \tag{2.17}$$

$\angle a_i^n(\omega)$ represents the argument of $a_i^n(\omega)$ for $i = 1, 2$, and $p_{0,n}^+$, $p_{0,n}^-$, $q_{0,n}^+$, $q_{0,n}^-$ are the smallest integers such that the corresponding $\tau_{n,p}^+(\omega)$, $\tau_{n,p}^-(\omega)$, $\sigma_{n,q}^+(\omega)$, $\sigma_{n,q}^-(\omega)$ are nonnegative. Since $\angle a_i$ and θ_i are continuous functions of ω on Ω_n, $i = 1, 2$, it follows that $\mathcal{T}_{n,p,q}^{\pm}(\omega)$ is also continuous on Ω_n for any n, p and q. We remark that, the method developed in [11] is also applicable to (2.5) for deriving the expression of the crossing curves.

Now we are ready to give a precise description of the mode-n crossing curve Π_n in the two cases: (i) $D_1 < |D_2|u^*$, and (ii) $D_1 > |D_2|u^*$.

Proposition 2.5. *If $D_1 < |D_2|u^*$, then there exists $N_1 \in \mathbb{N}$ such that, for any $n > N_1$, the mode-n crossing curve Π_n of (2.5) is a sequence of spiral-like curves in (τ, σ)-plane, oriented along σ-axis, that is, for each fixed p and n, Π_n is a spiral-like curve that extends infinitely along σ-axis but is bounded in the direction of τ-axis. Moreover, Π_n does not intersect with the σ-axis.*

Proof. When $D_1 < |D_2|u^*$, by (2) in proposition 2.4, there exists $N_1 \in \mathbb{N}$ such that $\Omega_n = [\omega_n^l, \omega_n^r]$ for $n > N_1$. Since $F_2^n(\omega_n^l) = F_1^n(\omega_n^r) = 1$, one can show that

$$\theta_1^n(\omega_n^l) = 0,\ \theta_2^n(\omega_n^l) = \pi,\ \theta_1^n(\omega_n^r) = \theta_2^n(\omega_n^r) = 0.$$

Therefore, $\mathcal{T}_{n,p,q}^+(\omega)$ is connected with $\mathcal{T}_{n,p,q-1}^-(\omega)$ at $\omega = \omega_n^l$, and $\mathcal{T}_{n,p,q}^+(\omega)$ is connected with $\mathcal{T}_{n,p,q}^-(\omega)$ at $\omega = \omega_n^r$. For fixed p and n, the set $\{\mathcal{T}_{n,p,q}^{\pm}(\omega) : q = q_{0,n}^{\pm}, q_{0,n}^{\pm} + 1, q_{0,n}^{\pm} + 2, \cdots\}$ forms a spiral-like curve, oriented along σ-axis. The other components of the crossing curve Π_n can be obtained by varying the index p from $p_{0,n}^{\pm}$ to ∞.

It follows from (2.16) that

$$\lim_{n\to\infty} a_1^n(\mathrm{i}\omega) = \frac{D_2 u^*}{D_1 + \mathrm{i}\sqrt{(D_2u^*)^2 - D_1^2}},\ \lim_{n\to\infty} a_2^n(\mathrm{i}\omega) = 0, \tag{2.18}$$

from which we have $\lim_{n\to\infty} |a_1^n(\mathrm{i}\omega)| = 1$ and $\lim_{n\to\infty} |a_2^n(\mathrm{i}\omega)| = 0$. Hence, $\lim_{n\to\infty} \theta_1^n(\omega) = 0$. This implies that $\tau_{n,p}^{\pm}(\omega)$ does not change sign on Ω_n for any fixed p and large n. □

By using proposition 2.5, we obtain the instability of the constant equilibrium $u = u^*$ when $D_1 < |D_2|u^*$ as follows.

Theorem 2.6. *Suppose that $(H1)$ and $(H2)$ are satisfied, and $D_1 < |D_2|u^*$. Then for any $\tau > 0$ and $\sigma \geqslant 0$, the constant equilibrium $u = u^*$ is linearly unstable with infinitely many pairs of complex roots with positive real parts.*

Proof. From proposition 2.5, there exists a sequence of spiral-like crossing curves of (2.5) for large n, oriented along σ-axis. In addition, the crossing curve that is closest to σ-axis is given by $\{\mathcal{T}_{n,p_{0,n}^{\pm},q}^{\pm}(\omega) : q = q_{0,n}^{\pm}, q_{0,n}^{\pm} + 1, q_{0,n}^{\pm} + 2, \cdots\} := \Lambda_n$. We show that Λ_n approaches σ-axis as $n \to \infty$. Recall that $\angle a_1^n(\mathrm{i}\omega)$ and $\theta_1^n(\omega)$ are bounded for $\omega > 0$. Since $\omega \in \Omega_n$ and $\omega_n^l \to \infty$, it follows from the first equation of (2.17) that $\tau_{n,p}^{\pm}(\omega) \to 0$ for any $\omega \in \Omega_n$, as $n \to \infty$. This implies that for any (τ, σ) with $\tau > 0$, $(\tau, \sigma) \notin \Theta_n$ for large n. Then $\Theta = \bigcap_{n=0}^{\infty} \Theta_n$ is an empty set, hence the constant equilibrium $u = u^*$ is linearly unstable with infinitely many pairs of complex roots with positive real parts. □

For $\sigma = 0$, it has been proved in [23] that (2.5) always have infinitely many complex roots, concentrated on the vertical line $\left\{z \in \mathbb{C} : \mathrm{Re} z = \ln \frac{|D_2|u^*}{D_1}\right\}$ in the complex plane. This implies that the constant equilibrium u^* is not stable for any $\tau > 0$ when $|D_2|u^* > D_1$. Theorem 2.6 shows that this is also the case for any $\sigma > 0$.

Next we consider the stability of u^* under the assumption $D_1 > |D_2|u^*$. We have the following result in that case.

Proposition 2.7. *Suppose that* $(H1)$ *and* $(H2)$ *are satisfied, and* $D_1 > |D_2|u^*$. *Then for* $n \in \mathbb{N}$,

(1) if

$$|D_2|u^*\lambda_n + |B| \leqslant |D_1\lambda_n - A|, \tag{2.19}$$

the mode-n crossing curve Π_n *of (2.5) is an empty set.*

(2) if

$$|D_2|u^*\lambda_n + |B| > |D_1\lambda_n - A|, \text{ and } |D_2|u^*\lambda_n - |B| > |D_1\lambda_n - A|, \tag{2.20}$$

the mode-n crossing curve Π_n *of (2.5) is a series of spiral-like curves, oriented along* σ*-axis;*

(3) if

$$|D_2|u^*\lambda_n + |B| > |D_1\lambda_n - A|, \text{ and } |D_2|u^*\lambda_n - |B| < -|D_1\lambda_n - A|, \tag{2.21}$$

the mode-n crossing curve Π_n *of (2.5) is a series of spiral-like curves, oriented along* τ*-axis; furthermore, let* $\sigma_*(D_2)$ *be the minimum of the* σ*-component of* $\{\mathcal{T}^{\pm}_{n,p,q^{\pm}_{0,n}}(\omega) : p = p^{\pm}_{0,n}, p^{\pm}_{0,n} + 1, p^{\pm}_{0,n} + 2, \cdots\}$, *which is the crossing curve closest to the* τ*-axis, then* $\frac{\mathrm{d}\sigma_*(D_2)}{\mathrm{d}D_2} < 0$.

(4) if

$$\begin{aligned} &|D_2|u^*\lambda_n + |B| > |D_1\lambda_n - A|, \\ \text{and } &-|D_1\lambda_n - A| < |D_2|u^*\lambda_n - |B| < |D_1\lambda_n - A|, \end{aligned} \tag{2.22}$$

the mode-n crossing curve Π_n *of (2.5) is open-ended; furthermore, assume that* $D_1\lambda_n - A > 0$, *and let* $\sigma^*(D_2)$ *be the minimum of the* σ*-component of* $\{\mathcal{T}^{\pm}_{n,p,q^{\pm}_{0,n}}(\omega) : p = p^{\pm}_{0,n}, p^{\pm}_{0,n} + 1, p^{\pm}_{0,n} + 2, \cdots\}$, *which is the crossing curve closest to the* τ*-axis, then* $\frac{\mathrm{d}\sigma^*(D_2)}{\mathrm{d}D_2} < 0$. *Here* $\sigma^*(D_2) = \sigma^{\pm}_{n,q}(\omega^r_n(D_2))$ *where* $\omega^r_n(D_2)$ *is the unique positive root of* $F^n_1(\omega) = 1$.

Proof. (1) is directly from part (1) of proposition 2.4, and for (2), the proof is similar to that of theorem 2.5, hence it is omitted here.

(3) By exchanging the two delays τ and σ, the existence of crossing curves follows directly from (2). Define

$$f(\sigma, s) := \mathrm{i}\frac{s}{\sigma} + D_1\lambda_n - A - B\mathrm{e}^{-\mathrm{i}s}, \text{ and } \Gamma_{D_2} := \{z \in \mathbb{C} : |z| = |D_2|u^*\lambda_n\}.$$

It follows from [11, theorem 3.2] that there exist $0 < \sigma_0(D_2) < \sigma_1(D_2) \leqslant \infty$ and $s_0(D_2), s_1(D_2) \in (0, \pi)$ such that

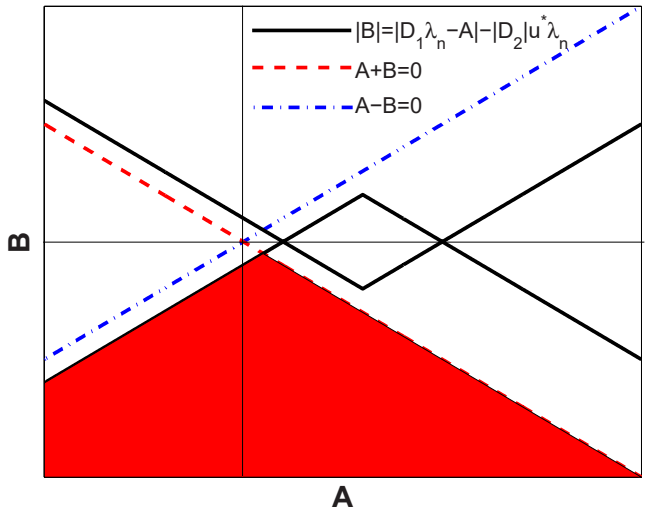

Figure 1. For fixed λ_n, the region of (A, B) for pattern formation in the case of $D_1 > |D_2|u^*$. The value of (A, B) in colored region, enclosed by the lines: $A + B = 0$, $A - B = 0$ and $|D_2|u^*\lambda_n + |B| = |D_1\lambda_n - A|$, satisfies (2b) in theorem 2.8.

$$f(\sigma_i(D_2), [0, \pi]) \cap \Gamma_{D_2} = \{f(\sigma_i(D_2), s_i(D_2))\}, \quad i = 0, 1,$$
$$f(\sigma, [0, \pi]) \cap \Gamma_{D_2} = \emptyset, \quad \sigma \in [0, \sigma_0(D_2)) \cup (\sigma_1(D_2), \infty),$$

and for fixed $\sigma \in (\sigma_0(D_2), \sigma_1(D_2))$, the curve $f(\sigma, s)$, $s \in [0, \pi]$, intersects Γ_{D_2} exactly twice. By [11, theorem 3.3], we know that $\sigma_*(D_2) = \sigma_0(D_2)$. Since the curve $f_\sigma(s)$ moves strictly downwards in the complex plane as σ increases. Therefore, $\sigma_0(D_2)$ is a decreasing function of D_2.

(4) By (2.22) and proposition 2.4, we have $\Omega_n = (0, \omega_n^r(D_2)]$, where $\omega_n^r(D_2)$ is the unique positive root of $F_1^n(\omega) = 1$. When $\omega = \omega_n^r(D_2)$, we conclude that $\theta_1^n(\omega) = \theta_2^n(\omega) = 0$. Thus, $\mathcal{T}_{n,p,q}^+(\omega)$ is connected with $\mathcal{T}_{n,p,q}^-(\omega)$ at this end. On the other hand, from (2.17), we know that $\mathcal{T}_{n,p,q}^\pm(\omega)$ approaches ∞ with different slopes, as $\omega \to 0$. Therefore, for fixed n, p, q, $\mathcal{T}_{n,p,q}^\pm(\omega)$ is an open-ended curve (or V-shaped curve) in (τ, σ)-plane. This proves the first statement.

From the expression of $F_1^n(\omega)$, it follows that $\omega_n^r(D_2)$ is a strictly increasing function of D_2. On the other hand, $\angle a_2^n(\mathrm{i}\omega_n^r(D_2)) = \arctan \frac{-\omega_n^r(D_2)}{D_1\lambda_n - A}$, which is a strictly decreasing function of D_2. If the minimum of $\sigma_{n,q}^\pm(\omega)$ is achieved at $\omega = \omega_n^r(D_2)$, then $\sigma^*(D_2) := \min_{D_2} \sigma_{n,q}^\pm(\omega) = \sigma_{n,q}^\pm(\omega_n^r(D_2)) = \frac{\angle a_2^n(\mathrm{i}\omega_n^r(D_2)) + (2q-1)\pi}{\omega_n^r(D_2)}$ decreases as D_2 increases. □

Now according to the crossing curve analysis in proposition 2.7, we arrive at the following stability result of the constant equilibrium u^* in the case of $D_1 > |D_2|u^*$.

Theorem 2.8. *Suppose that* $(H1)$ *and* $(H2)$ *are satisfied, and* $D_1 > |D_2|u^*$. *Then,*

(1) If $A + B < 0$, $B \geqslant A$, *then* u^* *is linearly stable for any* $\tau, \sigma \geqslant 0$; *that is,* $\Theta = \emptyset$;
(2) For $A + B < 0$, $B < A$, *we have*

(2a) If $|D_2|u^*\lambda_n + |B| < |D_1\lambda_n - A|$ *for each* $n \in \mathbb{N}$, *then for any* $\tau \geqslant 0$, *there exists* $\sigma_0 > 0$ *such that,* u^* *is linearly stable when* $\sigma < \sigma_0$ *and it is linearly unstable when* $\sigma > \sigma_0$*; that is,* $\Theta = \{(\tau, \sigma) : \tau \geqslant 0, \sigma_0 > \sigma \geqslant 0\}$*;*

(2b) If $|D_2|u^*\lambda_n + |B| > |D_1\lambda_n - A|$ *for some* $n \in \mathbb{N}$, *then* $\Theta \neq \emptyset$ *and* u^* *is linearly stable for* $(\tau, \sigma) \in \Theta$*; moreover* Θ *is determined by* Π_n *in proposition 2.7, depending on which condition (2.20), (2.21) or (2.22) is satisfied, and* Θ_0 *in proposition 2.3; if in addition, (2.21) or (2.22) is satisfied, then there exists* $D_2^* > 0$ *such that for* $0 < |D_2| < D_2^*$ *and any* $\tau \geqslant 0$, u^* *is linearly stable when* $\sigma < \sigma_0$, *and for* $|D_2| > D_2^*$, u^* *is linearly stable when* $(\tau, \sigma) \in \Theta$, *where the boundary of* Θ *is determined by* Π_n *in proposition 2.7 and* Θ_0 *in proposition 2.3.*

Proof. From $A + B < 0$, $B \geqslant A$ and $D_1 > |D_2|u^*$, we have $|D_2|u^*\lambda_n + |B| < |D_1\lambda_n - A|$ for each $n \in \mathbb{N}$. It then follows from proposition 2.4 that $\Omega_n = \emptyset$. Thus $\Sigma_n(\tau, \sigma) \subseteq \mathbb{C}^-$ for each $n \in \mathbb{N}$, and the stability of u^* is completely determined by (2.5) with $n = 0$. By proposition 2.3, we have $\Theta_0 = \{(\tau, \sigma) : \tau \geqslant 0, \sigma \geqslant 0\}$. This proves part (1) of the theorem.

For $A + B < 0, B < A$, from proposition 2.3, we know that $\Theta_0 = \{(\tau, \sigma) : \tau \geqslant 0, 0 \leqslant \sigma < \sigma_0\}$. If $|D_2|u^*\lambda_n + |B| < |D_1\lambda_n - A|$ for each $n \in \mathbb{N}$, then one can show part (2a) by a similar argument as above.

If $|D_2|u^*\lambda_n + |B| > |D_1\lambda_n - A|$ for some $n \in \mathbb{N}$ (see figure 1), one of conditions (2.20)–(2.22) is satisfied. From proposition 2.7, it concludes that the crossing curve Π_n is either spiral-like or open-ended, which determines the mode-n stability region Θ_n for u^*. On the other hand, by part (1) of proposition 2.4, we know that when $D_1 > |D_2|u^*$, there exists $N_2 \in \mathbb{N}$ such that all the roots of (2.5) have strictly negative real parts for any $n > N_2$. Therefore, the intersection of Θ_i for $0 \leqslant i \leqslant N_2$ determines the stability region Θ of u^*.

In the case of (2.21) and (2.22), the crossing curves are spiral-like curves oriented along τ-axis and open-ended curves, respectively. Furthermore, in either case, the minimum $\sigma_*(D_2)$ (or $\sigma^*(D_2)$) of σ-component of Π_n is a decreasing function of D_2, from proposition 2.7. Thus, there exists a unique $D_2^* > 0$ such that all the crossing curves of (2.5) with $n \geqslant 1$ and $D_2 \in (0, D_2^*)$ are above the line $\Pi_0 = \{(\tau, \sigma) : \tau \geqslant 0, \sigma = \sigma_0\}$, and therefore, $\Theta = \Theta_0$ when $D_2 \in (0, D_2^*)$. On the other hand, when $D_2 > D_2^*$, the stability region Θ depends on both Θ_0 and Θ_i for $1 \leqslant i \leqslant N_2$. This completes the proof of part (2b). □

Theorems 2.6 and 2.8 give a complete picture of stability property of the constant equilibrium $u = u^*$ of (1.2). First of all, when the memory-based diffusion strength D_2 is strong ($D_1 < |D_2|u^*$), then the constant equilibrium $u = u^*$ is unstable for all values of delays $\tau > 0$, $\sigma \geqslant 0$. When the memory-based diffusion strength D_2 is not strong ($D_1 > |D_2|u^*$), the relative magnitudes of the instantaneous growth rate $A = g_u(u^*, u^*)$ and delayed growth rate $B = g_{u_\sigma}(u^*, u^*)$ play a role in stability: the constant equilibrium u^* always remains stable if $A + B < 0$ and $A - B \leqslant 0$, which is in consistence with the case of $n = 0$ (proposition 2.3 part (1)). So a stability switch only occurs when $D_1 > |D_2|u^*$, $A + B < 0$ and $A - B > 0$. When D_2 is weak ($|D_2| < D_2^*$), then the constant equilibrium $u = u^*$ can only lose the stability to a spatially homogeneous (mode-0) time-periodic solution when $\sigma > \sigma_0$. The interesting case is in the intermediate strength D_2 of the memory-based diffusion ($D_2^* < |D_2| < D_1/u^*$), and the intersection of the crossing curves of (2.5) for some $n \in \mathbb{N}$ and Π_0 is nonempty. This implies that the boundary of Θ consists of two components: one is the line $\Pi_0 := \{(\tau, \sigma) : \tau \geqslant 0, \sigma = \sigma_0\}$, and the other part is determined by the crossing curves of (2.5) for some positive $n \in \mathbb{N}$. In this case, if (τ, σ) crosses $\partial\Theta \backslash \Pi_0$, then (2.5) has complex roots with $n \neq 0$ crossing the imaginary axis. As a result, a mode-n spatially inhomogeneous periodic orbit may bifurcate from the constant equilibrium u^* through a Hopf bifurcation.

Finally, we determine the direction in which the roots of (2.5) cross the imaginary axis, as (τ,σ) deviates from the boundary of Θ. As in [9], we called the direction of crossing curve that corresponds to increasing ω *the positive direction*. The region on the left hand side as we head in the positive direction of the crossing curve is called *the region on the left*.

Proposition 2.9. *Let $\omega\in\Omega_n$ and $(\tau,\sigma)\in\mathcal{T}^{\pm}_{n,p,q}$ such that $\mu=\mathrm{i}\omega$ is a simple root of $E(n,\tau,\sigma,\mu)=0$ in the sense that $E(n,\tau,\sigma,\mathrm{i}\omega')\neq 0$ for any $\omega'>0$ and $\omega'\neq\omega$. Then, as (τ,σ) moves from the region on the right to the region on the left of the crossing curve, a pair of complex roots of (2.5) cross the imaginary axis to the right if*

$$BD_2\sin(\omega(\tau-\sigma))>0. \tag{2.23}$$

The crossing is in the opposite direction if the (2.23) is reversed.

Proof. By proposition 6.1 in [9], it suffices to show that (2.23) is equivalent to $R_2I_1-R_1I_2>0$, where

$$\begin{aligned}
R_1&:=-\mathrm{Re}\left(\frac{1}{\mu}\frac{\partial a^n(\mu,\tau,\sigma)}{\partial\tau}\right)_{\mu=\mathrm{i}\omega}=\mathrm{Re}(a_1^n(\mathrm{i}\omega)\mathrm{e}^{-\mathrm{i}\omega\tau})=\frac{B_n}{A_n^2+\omega^2}(A_n\cos\omega\tau-\omega\sin\omega\tau),\\
R_2&:=-\mathrm{Re}\left(\frac{1}{\mu}\frac{\partial a^n(\mu,\tau,\sigma)}{\partial\sigma}\right)_{\mu=\mathrm{i}\omega}=\mathrm{Re}(a_2^n(\mathrm{i}\omega)\mathrm{e}^{-\mathrm{i}\omega\sigma})=\frac{-B}{A_n^2+\omega^2}(A_n\cos\omega\sigma-\omega\sin\omega\sigma),\\
I_1&:=-\mathrm{Im}\left(\frac{1}{\mu}\frac{\partial a^n(\mu,\tau,\sigma)}{\partial\tau}\right)_{\mu=\mathrm{i}\omega}=\mathrm{Im}(a_1^n(\mathrm{i}\omega)\mathrm{e}^{-\mathrm{i}\omega\tau})=\frac{-B_n}{A_n^2+\omega^2}(\omega\cos\omega\tau+A_n\sin\omega\tau),\\
I_2&:=-\mathrm{Im}\left(\frac{1}{\mu}\frac{\partial a^n(\mu,\tau,\sigma)}{\partial\sigma}\right)_{\mu=\mathrm{i}\omega}=\mathrm{Im}(a_2^n(\mathrm{i}\omega)\mathrm{e}^{-\mathrm{i}\omega\sigma})=\frac{B}{A_n^2+\omega^2}(\omega\cos\omega\sigma+A_n\sin\omega\sigma).
\end{aligned} \tag{2.24}$$

In fact, from (2.24), one can compute that

$$\mathrm{Sign}(R_2I_1-R_1I_2)=\mathrm{Sign}\frac{B_nB\sin(\omega(\tau-\sigma))}{A_n^2+\omega^2}=\mathrm{Sign}[BD_2\sin(\omega(\tau-\sigma))].$$

This completes the proof. □

We conclude this section with the following result regarding mode-n stability switch of the constant equilibrium u^*, which follows from theorem 2.8 and proposition 2.9.

Theorem 2.10. *Suppose that (H1) and (H2) are satisfied, $D_1>|D_2|u^*>0, A+B<0$ and $B<A$. If $|D_2|u^*\lambda_n+|B|>|D_1\lambda_n-A|$ for some $n\in\mathbb{N}$, then there exists $(\tau_0,\sigma_0)\in\partial\Theta\cap\Pi_n$ and $\omega_0\in\Omega_n$ for $n\in\mathbb{N}$. Moreover if $\omega_0(\sigma_0-\tau_0)\neq k\pi$ for $k\in\mathbb{Z}$ and $\mu=\mathrm{i}\omega_0$ is a simple root of $E(n,\tau_0,\sigma_0,\mu)=0$, then there exists a neighborhood U of (τ_0,σ_0) such that when $(\tau,\sigma)\in U\cap\Theta$, $u=u^*$ is locally asymptotically stable, and when $(\tau,\sigma)\in U\backslash\overline{\Theta}$, $u=u^*$ is unstable which has exactly two eigenvalues with positive real part.*

Theorem 2.10 provides a guidance of locating the pairs of delay values (τ,σ), diffusion coefficients (D_1,D_2) and growth rates (A,B) which produce spatiotemporal oscillatory patterns. In the next section we give a couple of examples and numerical simulations to demonstrate this mechanism of pattern formation.

3. Examples

In this section we apply our theory in section 2 to (1.2) with the Wright–Hutchinson form of delayed reaction and also some variants which are biologically more relevant.

3.1. Wright–Hutchinson form

A typical choice of the delayed growth function in (1.2) is the logistic one in the Wright–Hutchinson equation $g(u,u_\sigma)=ru\left(1-\frac{u_\sigma}{K}\right)$. Let

$$\tilde{u}=\frac{u}{K},\ \tilde{t}=rt,\ \tilde{x}=x\left(\frac{r}{D_1}\right)^{1/2},$$

and rescale the parameters via

$$D=\frac{KD_2}{D_1},\ \tilde{\tau}=\tau r,\ \tilde{\sigma}=\sigma r.$$

This gives rise to the following nondimensionalized system of (1.2), after dropping the tildes:

$$\begin{cases}\frac{\partial u}{\partial t}=\Delta u+D\,\mathrm{div}(u\nabla u(t-\tau,x))+u(1-u(t-\sigma,x)), & x\in\Omega,t>0,\\ \frac{\partial u}{\partial n}(t,x)=0, & x\in\partial\Omega,t>0.\end{cases}\tag{3.1}$$

It is apparent that $u^*=1$ is the unique positive constant equilibrium, and $A=g_u(u^*,u^*)=0$, $B=g_{u_\sigma}(u^*,u^*)=-1$. Therefore,

$$A_n=\lambda_n,\ \ B_n=D\lambda_n.\tag{3.2}$$

If $n=0$, it is well-known that all the roots of (2.5), with A_n and B_n given in (3.2), have strictly negative real parts when $\sigma<\pi/2$ [24, 26, 32]. Hence, $\Theta_0=\{(\tau,\sigma):\tau\geqslant 0,\sigma\in(0,\pi/2)\}$. If $|D|>1$, it then follows from proposition 2.5 that the mode-n crossing curve Π_n consists of a sequence of spiral-like curves in (τ,σ)-plane, oriented along σ-axis, see figure 2. As a consequence of theorem 2.6, u^* is always linearly unstable for any $\tau,\sigma>0$, as long as $|D|>1$. In the case of $|D|<1$, theorem 2.8 tells that the stable region of (3.1) is given by Θ. We illustrate how to determine Θ in the following two examples.

Example 3.1. Let the spatial dimension $N=1$ and $\Omega=(0,l)$ with $l=5$ and $D=0.7$. Then, $\lambda_1\approx 0.3948$, $\lambda_2\approx 1.5791$ and $\lambda_3\approx 3.5531$. It can be verified that (2.21) holds for $n=1$, (2.22) is satisfied for $n=2$, and $|B_n|+|B|<|A_n|$ for any $n\geqslant 3$. From (1) of proposition 2.4, we know that $\Omega_n=\emptyset$ for $n\geqslant 3$, which implies that all the roots of (2.5) with (3.2) has strictly negative real parts for all $\tau,\sigma>0$ and $n\geqslant 3$.

It remains to determine the crossing curves for $n=1,2$. By proposition 2.7, the crossing curves of (2.5) with $n=1$ are a sequence of spiral-like curves, oriented along τ-axis in the complex plane, as shown by red solid curves in figure 3 (left). For $n=2$, it follows from proposition 2.7 that the associated crossing curves of (2.5) consist of a series of open-ended (or V-shaped) curves, see the blue dotted curves in figure 3 (left). Here, all these crossing curves are plotted with the aid of DDE-BIFTOOL, a MatLab package for numerical bifurcation and stability analysis of delay differential equations with several discrete and/or state-dependent delays, see [7].

These curves determine the stable region Θ, that is, the horizontal strip enclosed by the black line, τ- and σ-axis, but not including $R_1\cup R_2\cup R_3\cup\cdots$, see figure 3 (right). By theorem 2.8, we conclude that the constant steady state u^* is asymptotically stable for $(\tau,\sigma)\in\Theta$.

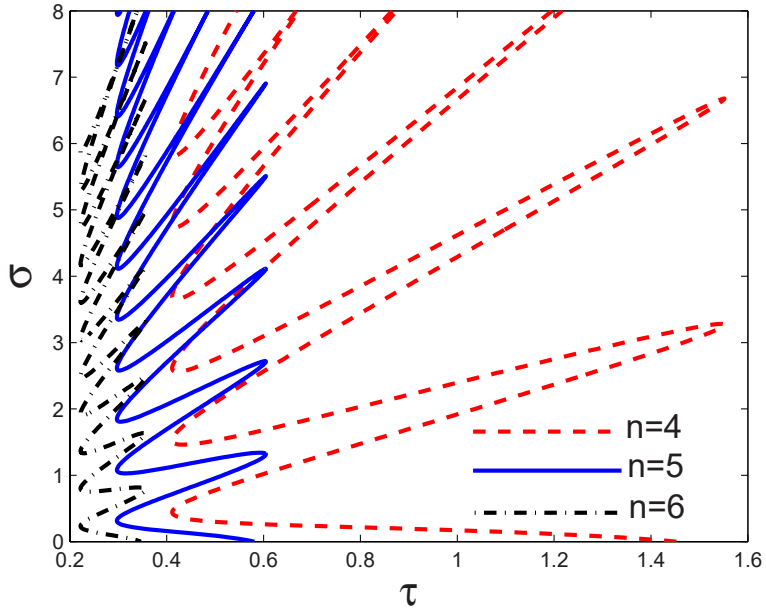

Figure 2. The mode-n crossing curves for (3.1) with large n in the case of $|D| > 1$. Here, $\Omega = (0, 5)$ and $D = 1.2$.

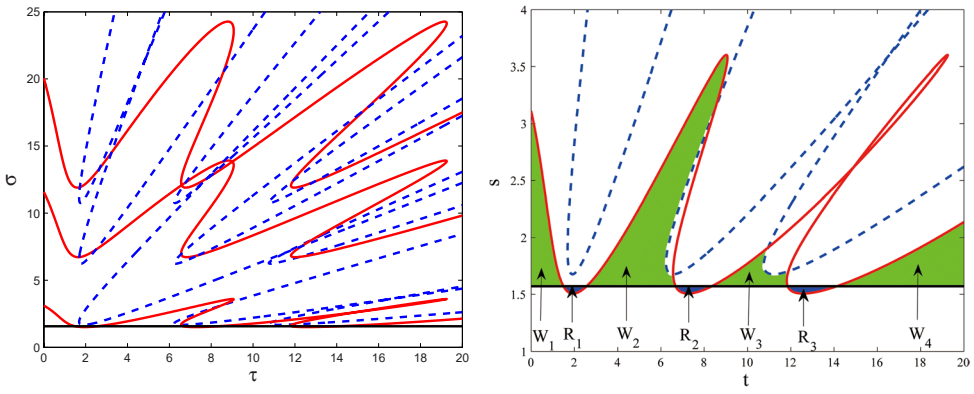

Figure 3. The mode-n crossing curves for (3.1) in the case of $|D| < 1$ for $n = 0, 1, 2$. Here $\Omega = (0, 5)$ and $D = 0.7$. Left: crossing curves for (3.2) with $n = 0$ (black solid), $n = 1$ (red solid) and $n = 2$ (blue dotted); right: zoom-in of the bottom for left graph.

Furthermore, for $(\tau, \sigma) \in R_1 \cup R_2 \cup R_3 \cup \cdots$, a spatially inhomogeneous periodic solution can be observed (figure 4 (left)); while for $(\tau, \sigma) \in W_1 \cup W_2 \cup W_3 \cup \cdots$, the observed periodic solution is spatially homogeneous (figure 4 (right)). It is also remarked that there exists a $\bar{\sigma} > 0$ such that the equilibrium is stable for all $\tau > 0$ when $0 < \sigma < \bar{\sigma}$.

If D is decreased to 0.5, then the crossing curves for (2.5) with $n = 1, 2$ are slightly different from the ones for $D = 0.7$. It can be seen that the bottom red crossing curve for $n = 1$ will never intersect the one for $n = 0$ (black solid line), see figure 5 (left). Therefore, u^* is stable for (τ, σ) within the rectangle region below the black solid line, and a spatially homogeneous periodic solution of (3.1) exists for (τ, σ) lying in R (the region between the red and black

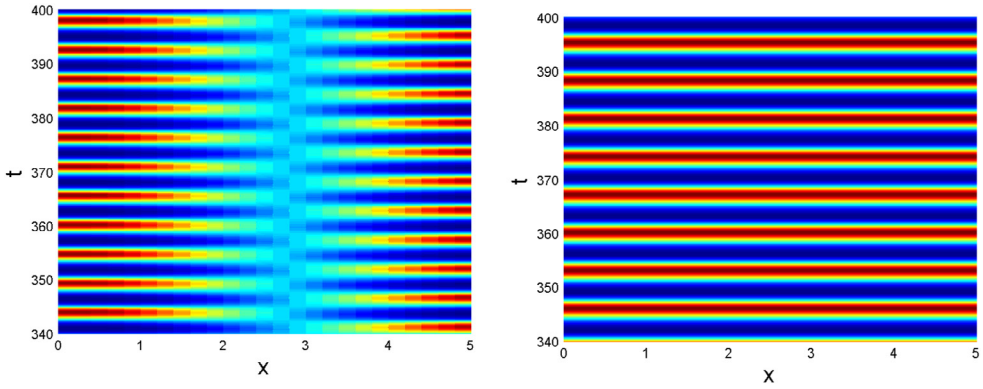

Figure 4. Periodic solutions of (3.1) with different delays. Left: a spatially inhomogeneous periodic solution for $(\tau,\sigma)=(2,1.52)\in R_1$; right: a spatially homogeneous periodic solution for $(\tau,\sigma)=(1,1.7)\in W_1$. Here, $\Omega=(0,5)$, $D=0.7$ and the initial function $u(\theta,x)=1+0.1\cos(\pi x/5)$ for $\theta\in[-\tau,0]$.

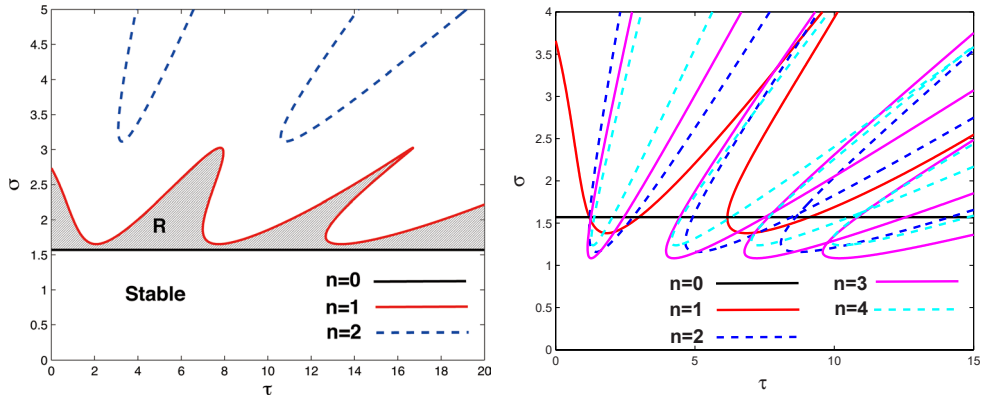

Figure 5. The mode-n crossing curves for (3.1) in the case of $|D|<1$. Here $\Omega=(0,5)$, $D=0.5$ (left) and $D=0.9$ (right).

curve). This is verified in (2b) of theorem 2.8 that when $|D_2|<D_2^*$, the stability switch only occurs for $n=0$ thus there is no spatiotemporal pattern generated in this case.

Next we let $D=0.9$. The crossing curves in this case are much more complicated than the case of $D=0.7$ or $D=0.5$, see figure 5 (right). In this situation, spatiotemporal patterns of (3.1) with higher mode-n are also observed, see figure 6. When $D=0.95$, figure 7 shows a spatiotemporal pattern with sharper transition layers between different phases.

Example 3.2. Let the spatial dimension $N=2$ and $\Omega=(0,l)\times(0,l)$. Then the eigenvalues are $\lambda_{m,n}=\frac{(m^2+n^2)\pi^2}{l^2}$ for $m,n\in\mathbb{N}_0$. Set $l=5$ and $D=0.8$. It can be verified that $|B_{m,n}|+|B|<|A_{m,n}|$ if $m^2+n^2>12$, where $A_{m,n}=\lambda_{m,n}$ and $B_{m,n}=D\lambda_{m,n}$. This implies that all the roots of (2.5) have negative real parts for $m^2+n^2>12$. For $m^2+n^2<12$ and $m,n\in\mathbb{N}$, (2.22) is satisfied. It follows from proposition 2.7 that all the crossing curves are open ended. All these curves can be plotted as in previous example, and their graphs are similar to the ones in figure 3 (right) and figure 5, which are omitted here. Since some crossing curves intersect Θ_0, if we further assume $\sigma<\pi/2$, then the memory diffusive delay τ also

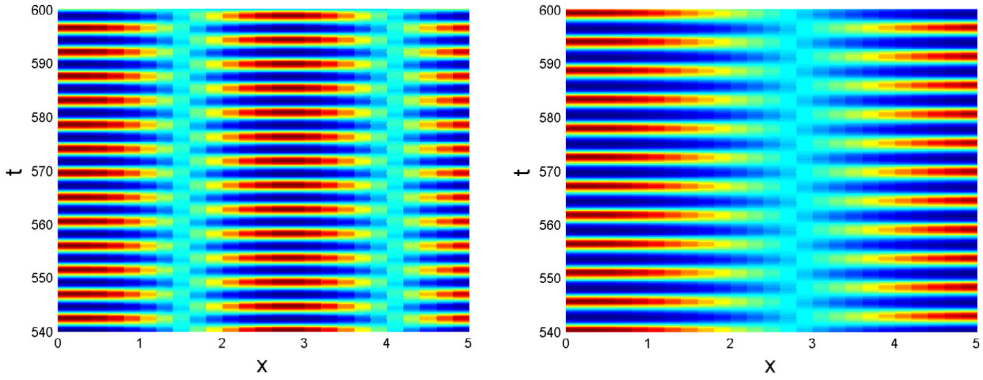

Figure 6. Spatially inhomogeneous periodic solutions of (3.1) with different delays. Here $D = 0.9$ and $\tau = 2$, and $\sigma = 1.35$ (left) or $\sigma = 1.5$ (right). All other parameters and initial conditions are same as the ones in figure 4.

leads to the existence of purely imaginary roots of (2.5) with (3.2) for some $n \neq 0$. In this case, a spatially inhomogeneous periodic solution of (3.1) bifurcates from the constant equilibrium u^*, as (τ, σ) passing through the crossing curve from the stable region Θ, see figure 8.

We remark that all the spatially inhomogeneous periodic solutions in previous two examples are plotted for $0 < \sigma < \pi/2$ where spatially homogeneous periodic solutions do not exist. This reveals that such solutions are caused by the memory-based diffusion delay τ (due to the existence of purely imaginary roots of (2.5) for some $n \geqslant 1$). In [23], it was shown that the memory-based diffusion delay τ does not play a role in pattern formation in the case of $\sigma = 0$.

3.2. Corrected Wright–Hutchinson form

The Wright–Hutchinson equation (3.1) is classical but also controversial, because the second term includes both non-delayed and delayed dependent variables. However one event can only occur at one moment. Actually, the quadratic term from the logistic model is normally interpreted as self-crowding effect. The delay can be interpreted in many different ways, but almost all of them lead to a delay in the birth term because it takes a long time for renewable resources or newly-born animals or newly-divided cells to reach maturity for reproduction or cell division. As a conclusion, the delayed logistic equation should be corrected as

$$u'(t) = bu(t-\sigma) - cu^2(t), \tag{3.3}$$

where b is the birth rate and c is the crowding effect parameter, which describes the competition for space or some limiting resources. If we further consider the natural death, then the equation becomes

$$u'(t) = bu(t-\tau_2) - du(t) - cu^2(t). \tag{3.4}$$

When the factors of random and memory-based diffusions are incorporated, (3.4) becomes

$$\frac{\partial u}{\partial t} = D_1 \Delta u + D_2 \operatorname{div}(u \nabla u(t-\tau_1, x)) + bu(t-\tau_2, x) - du(t,x) - cu^2(t,x).$$

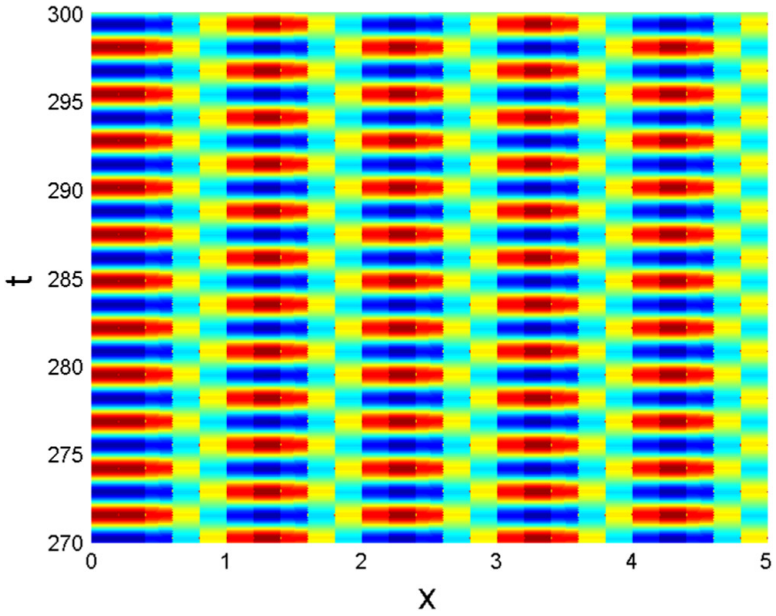

Figure 7. A spatially inhomogeneous periodic solution of (3.1) with $D = 0.95, \tau = 1.18$ and $\sigma = 1.5$. All other parameters and initial conditions are same as the ones in figure 4.

After re-scaling parameters, that is,

$$\tilde{u} = \frac{bu}{c},\ \tilde{t} = bt,\ \tilde{x} = x\left(\frac{b}{D_1}\right)^{1/2},$$

we have

$$\frac{\partial u}{\partial t} = \Delta u + D\,\mathrm{div}(u\nabla u(t-\tau,x)) + u(t-\sigma,x) - ru(t,x) - u^2(t,x), \tag{3.5}$$

where

$$D = \frac{bD_2}{cD_1},\ r = \frac{d}{b},\ \tau = b\tau_1,\ \sigma = b\tau_2. \tag{3.6}$$

It is straightforward that (3.5) admits a unique constant equilibrium $u^* = 1 - r$ for $r < 1$, and $A = g_u(u^*, u^*) = r - 2 < 0,\ B = g_{u_\sigma}(u^*, u^*) = 1$. Therefore, $A + B < 0$ and $B > A$. From theorems 2.6 and 2.8, we know that if $D(1 - r) < 1$ (or $D(1 - r) > 1$), u^* is always stable (or unstable) for $\sigma, \tau \geqslant 0$.

In general, from the idea in [20], (3.4) can be extended to the following more general model:

$$u'(t) = bu(t-\tau_2)f(u(t-\tau_2)) - du(t) - cu^2(t). \tag{3.7}$$

There are many options for the birth function f in the literature, such as

$$f(u(t-\tau_2)) = \frac{1}{1+\beta u(t-\tau_2)} \text{ or } f(u(t-\tau_2)) = u^\alpha(t-\tau_2),$$

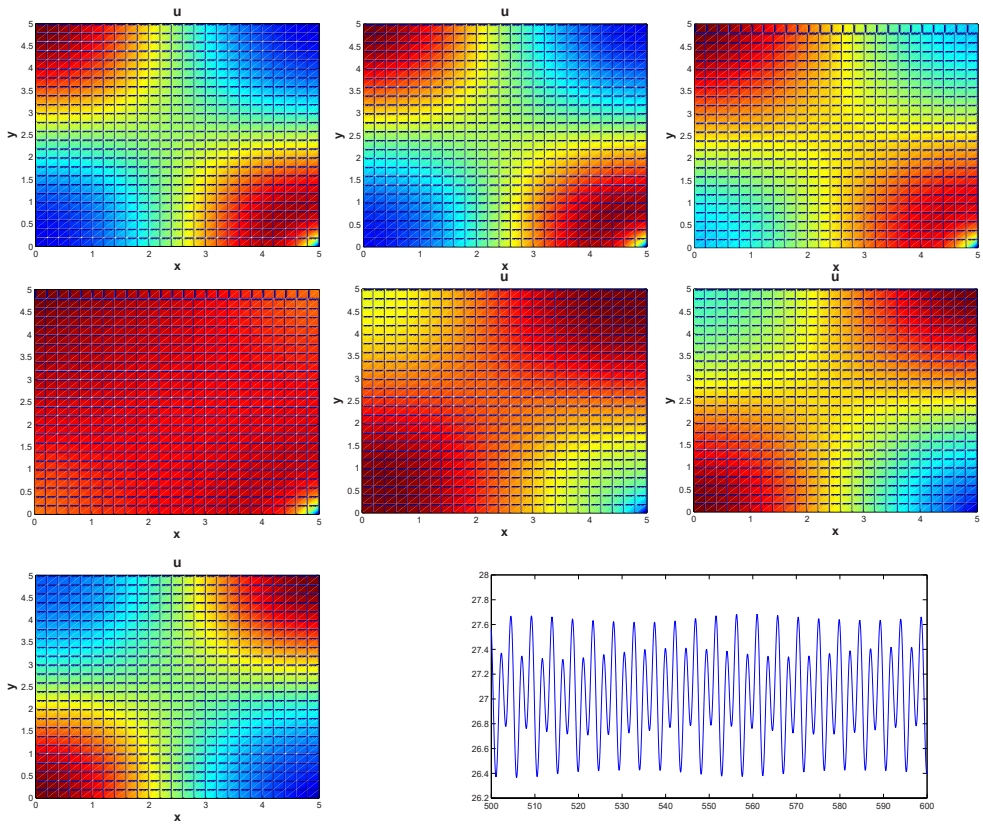

Figure 8. A spatially inhomogeneous periodic solution of (3.1) when $N = 2$. Here $\Omega = (0,5) \times (0,5)$, $D = 0.8$, $\tau = 1.7$ and $\sigma = 1.55$. The spatial snapshots in a spatially inhomogeneous periodic solution of (3.1) are plotted at different times, which is a half period as the first and last snapshots are anti-phased, and the last panel shows the variation of total mass of u with respect to t.

which are referred to Beverton–Holt type and Pascual type, respectively. Obviously, for Pascual type f with $\alpha = 0$, the equation (3.7) is same as the equation (3.4). For Beverton–Holt type f, the re-scaled equation of (3.7) is

$$\frac{\partial u}{\partial t} = \Delta u + D\,\mathrm{div}(u\nabla u(t-\tau,x)) + \frac{u(t-\sigma,x)}{1+\alpha u(t-\sigma,x)} - ru(t,x) - u^2(t,x) \tag{3.8}$$

where D, τ, σ, r are defined as in (3.6) and $\alpha = \frac{b\beta}{c}$. It can be verified that (3.8) has a unique positive steady state

$$u^* = \frac{-(1+\alpha r) + \sqrt{(1+\alpha r)^2 - 4\alpha(r-1)}}{2\alpha}$$

as long as $r < 1$. Furthermore, $A = g_u(u^*, u^*) = -(r + 2u^*) < 0$ and $B = g_{u_\sigma}(u^*, u^*) = \frac{1}{(1+\alpha u^*)^2} \in (0,1)$, which implies $B > A$. If $1 < (r + 2u^*)(1 + \alpha u^*)^2$, then $A + B < 0$. Using theorems 2.6 and 2.8 again, we conclude that if $Du^* < 1$ (or $Du^* > 1$), u^* is always stable

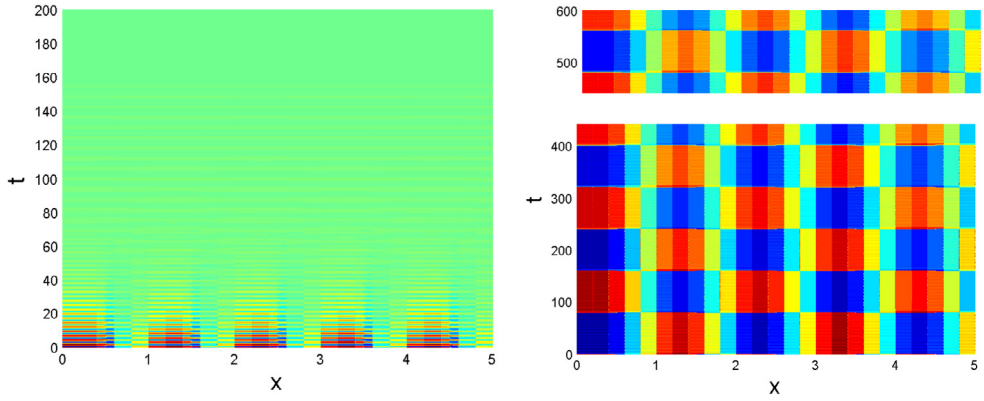

Figure 9. For (4.1), choose $g = ru\left(1 - \int_\Omega K(x,y)u(y,t-\sigma)\mathrm{d}y\right)$ with triangular distribution function $K(x,y)$ such that $\int_\Omega K(x,y)\mathrm{d}y = 1$ for any x. Here, $D_1 = 1$, $D_2 = 0.95$, $\sigma = 1.5$, $\Omega = (0,5)$ and $r = 1$. The constant equilibrium is stable for $\tau = 1.18$ (left); and periodic oscillation can be observed for $\tau = 80$ (right).

(or unstable) for $\sigma, \tau \geqslant 0$. Hence (3.5) or more generally (3.8) provides an example of (1.2) that cannot produce spatiotemporal oscillations, while (3.1) does.

4. Discussion

In this paper, we incorporate the maturation delay into the reaction–diffusion model with spatial memory, that was originally proposed in [23]. We show that the positive constant steady state is always unstable if the effect of memory-based diffusion is stronger than that of Fickian one, that is, $|D_2|u^* > D_1$, no matter how the memory diffusion delay τ and the maturation delay σ vary. This conclusion is similar to the one in the case of $\sigma = 0$, which has been studied in [23]. However, the situation is different when $|D_2|u^* < D_1$. Without memory-based diffusion, it is known that the change of the maturation delay σ can lead to Hopf bifurcation at any constant steady state, and the stable bifurcated periodic solution is spatially homogeneous. If the memory-based diffusion is involved, we can find all the crossing curves in (τ, σ)-plane, on which the characteristic equation has purely imaginary roots. Moreover, these curves determine the stable region Θ of (1.2). The boundary of Θ consists of two segments, where the system can give rise to spatially homogeneous and inhomogeneous periodic solutions through Hopf bifurcation, respectively. These results are illustrated numerically in examples.

It is also worth mentioning that the effects of diffusion and time delays are not independent of each other, i.e. the individuals located at x in previous time may move to another place at present. Thus, a more reasonable revision of (1.2) would be

$$\frac{\partial u}{\partial t} = D_1\Delta u + D_2\,\mathrm{div}(u\nabla u_\tau) + g\left(u, \int_\Omega K(x,y)u(t-\sigma,y)\mathrm{d}y\right), \tag{4.1}$$

which is an open problem as future work. The simulation results of the nonlocal reaction model (4.1), exhibited in figure 9, clearly show the departure from the local reaction model (1.2).

For the nonlocal reaction model (4.1), we further remark that the memory-based diffusion term involving the memory delay should be in local form, since animals move due to footprints or their memorized distribution τ time ago. Footprints cannot move, thus it is clear that

nonlocal effect is not relevant in this case. For memory-based diffusion, the decision-making animal moves according to its memorized distribution like using GPS navigation, although the present distribution of animals is different from the past distribution.

Acknowledgment

J P Shi's research is partially supported by NSF Grant DMS-1715651, C C Wang's research is partially supported by Chinese NSF Grant 11671110 and Heilongjiang NSF Grant LH2019A010, and H Wang's research is partially supported by an NSERC Grant.

References

[1] Bélair J and Campbell S A 1994 Stability and bifurcations of equilibria in a multiple-delayed differential equation *SIAM J. Appl. Math.* **54** 1402–24
[2] Busenberg S and Huang W 1996 Stability and hopf bifurcation for a population delay model with diffusion effects *J. Differ. Equ.* **124** 80–107
[3] Chen S S and Shi J P 2012 Stability and hopf bifurcation in a diffusive logistic population model with nonlocal delay effect *J. Differ. Equ.* **253** 3440–70
[4] Chen S S and Yu J S 2016 Stability analysis of a reaction–diffusion equation with spatiotemporal delay and Dirichlet boundary condition *J. Dynam. Differ. Equ.* **28** 857–66
[5] Chen S S and Yu J S 2016 Stability and bifurcations in a nonlocal delayed reaction–diffusion population model *J. Differ. Equ.* **260** 218–40
[6] Crank J 1979 *The Mathematics of Diffusion* (Oxford: Oxford University Press)
[7] Engelborghs K, Luzyanina T and Samaey G 2001 DDE-BIFTOOL v. 2.00: a Matlab package for bifurcation analysis of delay differential equations *Technical Report* tw-330, Department of Computer Science, K.U.Leuven, Leuven, Belgium
[8] Fagan W F *et al* 2013 Spatial memory and animal movement *Ecol. Lett.* **16** 1316–29
[9] Gu K, Niculescu S I and Chen J 2005 On stability crossing curves for general systems with two delays *J. Math. Anal. Appl.* **311** 231–53
[10] Guo S-J 2015 Stability and bifurcation in a reaction–diffusion model with nonlocal delay effect *J. Differ. Equ.* **259** 1409–48
[11] Hale J and Huang W 1993 Global geometry of the stable regions for two delay differential equations *J. Math. Anal. Appl.* **178** 344–62
[12] Kot M 2001 *Elements of Mathematical Ecology* (Cambridge: Cambridge University Press)
[13] Lin X and Wang H 2012 Stability analysis of delay differential equations with two discrete delays *Can. Appl. Math. Q.* **20** 519–33
[14] MacDonald N 1978 *Time Lags in Biological Models* (Berlin: Springer)
[15] Mahaffy J M, Joiner K M and Zak P J 1995 A geometric analysis of stability regions for a linear differential equation with two delays *Int. J. Bifur. Chaos Appl. Sci. Eng.* **5** 779–96
[16] Memory M 1989 Bifurcation and asymptotic behavior of solutions of a delay-differential equation with diffusion *SIAM J. Math. Anal.* **20** 533–46
[17] Murray J D 2003 *Mathematical Biology. II. Spatial Models and Biomedical Applications* (*Interdisciplinary Applied Mathematics* vol 18) 3rd edn (New York: Springer)
[18] Niculescu S-I, Kim P S, Gu K, Lee P P and Levy D 2010 Stability crossing boundaries of delay systems modeling immune dynamics in leukemia *Discrete Continuous Dyn. Syst.* B **13** 129–56
[19] Okubo A and Levin S A 2001 *Diffusion and Ecological Problems: Modern Perspectives* (*Interdisciplinary Applied Mathematics* vol 14) 2nd edn (New York: Springer)
[20] Pascual M, Roy M and Laneri K 2011 Simple models for complex systems: exploiting the relationship between local and global densities *Theor. Ecol.* **4** 211–22
[21] Piotrowska M J 2007 A remark on the ODE with two discrete delays *J. Math. Anal. Appl.* **329** 664–76
[22] Ruan S G and Wei J J 2003 On the zeros of transcendental functions with applications to stability of delay differential equations with two delays *Dyn. Continuous Discrete Impulsive Syst.* A **10** 863–74

[23] Shi J, Wang C, Wang H and Yan X 2019 Diffusive spatial movement with memory *J. Dynam. Differ. Equ.* (accepted) https://doi.org/10.1007/s10884-019-09757-y
[24] Shi J P 2013 Absolute stability and conditional stability in general delayed differential equations *Advances in Interdisciplinary Mathematical Research* (*Springer Proc. in Mathematics and Statistics* vol 37) (New York: Springer) pp 117–31
[25] Shi Q Y, Shi J P and Song Y L 2017 Hopf bifurcation in a reaction–diffusion equation with distributed delay and Dirichlet boundary condition *J. Differ. Equ.* **263** 6537–75
[26] Smith H 2011 *An Introduction to Delay Differential Equations with Applications to the Life Sciences* (*Texts in Applied Mathematics* vol 57) (New York: Springer)
[27] Su Y, Wei J J and Shi J P 2009 Hopf bifurcations in a reaction–diffusion population model with delay effect *J. Differ. Equ.* **247** 1156–84
[28] Su Y, Wei J J and Shi J P 2012 Hopf bifurcation in a diffusive logistic equatioin with mixed delayed and instantaneous density dependence *J. Dynam. Differ. Equ.* **24** 897–925
[29] Taylor M E 2010 *Partial Differential Equations* III (*Applied Mathematical Science* vol 117) 2nd edn (New York: Springer)
[30] Wei J J and Ruan S G 1999 Stability and bifurcation in a neural network model with two delays *Physica* D **130** 255–72
[31] Wu J H 1996 *Theory of Partial Functional Differential Equations* (Berlin: Springer)
[32] Yan X P and Shi J P 2017 Stability switches in a logistic population model with mixed instantaneous and delayed density dependence *J. Dynam. Differ. Equ.* **29** 113–30
[33] Yan X P and Li W T 2010 Stability of bifurcating periodic solutions in a delayed reaction–diffusion population model *Nonlinearity* **23** 1413–31
[34] Yi F Q, Wei J J and Shi J P 2009 Bifurcation and spatiotemporal patterns in a homogeneous diffusive predator-prey system *J. Differ. Equ.* **246** 1944–77
[35] Yoshida K 1982 The Hopf bifurcation and its stability for semilinear diffusion equations with time delay arising in ecology *Hiroshima Math. J.* **12** 321–48